SYNAPSE-SPECIFIC COINCIDENCE DETECTION BY VOLTAGE-GATED CALCIUM CHANNELS

HUGH T. BLAIR & DANIEL C. BOYAR
UCLA Dept. of Psychology, Los Angeles, CA (blair@psych.ucla.edu)

Abstract. It has been proposed that voltage-gated calcium channels (VGCCs) may function as coincidence detectors of simultaneous pre- and postsynaptic activity, by opening preferentially when postsynaptic backpropogating action potentials (BPAPs) are amplified by presynaptically generated excitatory postsynaptic potentials (EPSPs)[1,2]. Here we present simulations showing that when a BPAP collides with an EPSP, amplification of the BPAP is poorly localized to the synapse where the EPSP occurs. Nonetheless, the activation of VGCCs by the amplified BPAP is better localized to the region of the input synapse than the amplified BPAP itself, due to spatial filtering of the voltage signal by the VGCC activation threshold. This supports the idea that VGCCs may contribute to Hebbian coincidence detection.

Donald Hebb[3] proposed that when two interconnected neurons fire at the same time, the synapses between them become stronger, and remain stronger for a long time afterward. Such "Hebbian plasticity" requires a biological mechanism for coincidence detection of simultaneous activity between interconnected neurons. NMDA receptors are known to function as Hebbian coincidence detectors[4], but some forms of homosynaptic plasticity can occur without NMDA receptors, often requiring VGCCs instead[5-7]. These findings have led to the hypothesis that VGCCs may serve as Hebbian coincidence detectors under some circumstances, but since VGCCs are opened by postsynaptic depolarization independently of presynaptic activity, it remains unclear how VGCCs could be opened in a synapse-specific manner to support Hebbian plasticity. Here, we investigated this question using computer simulations.

Simulation Parameters

We used the NEURON simulator running on a Windows PC to construct a model of two neurons: a presynaptic cell and a postsynaptic cell (Fig. 1). Passive membrane parameters were uniform throughout both cells (R_i=150 Ωcm, C_m=1 μF/cm^2, and R_m=12 KΩcm^2). Hodgkin-Huxley Na^+ and K^+ channels were modeled as in Mainen et al.[8], with densities in the postsynaptic cell set to 30 pS/μm^2 and 50 pS/μm^2 in the soma and dendrites, and 15,000 pS/μm^2 and 500 30 pS/μm^2 in the axon, respectively[2]. Na^+ and K^+ channel densities in the presynaptic cell were 1200 pS/μm^2 and 300 pS/μm^2, respectively. Synaptic AMPA conductances were simulated using a two-state kinetic model[9], and NMDA conductances using a five-state kinetic model[10], both with reversal potential of 0 mV (see Fig. 2 caption for receptor densities). VGCCs were simulated using Hodgkin-Huxley kinetics, with n_∞ and τ_∞ curves fitted to experimental observations of L-type channels[11]. The half-activation threshold for VGCCs was $V½_\alpha$ = -14.25 mV. VGCC density was 10 pS/μm^2 in spine heads, and zero everywhere else. Ionic reversal potentials were E_{Na}=60 mV,

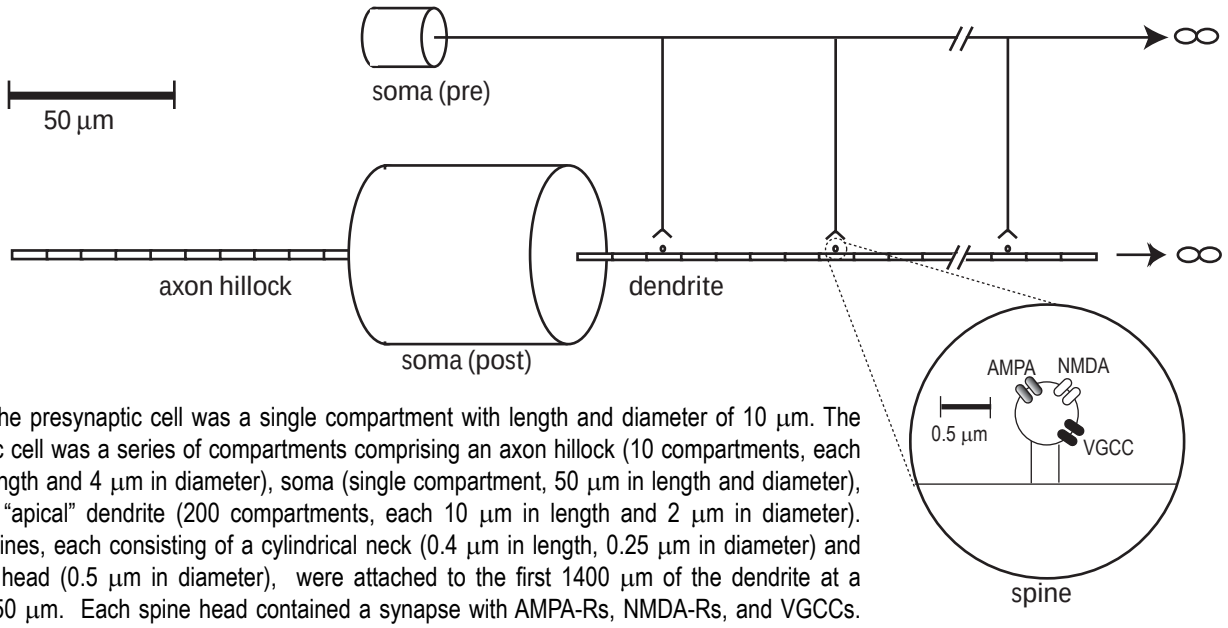

Figure 1. The presynaptic cell was a single compartment with length and diameter of 10 μm. The postsynaptic cell was a series of compartments comprising an axon hillock (10 compartments, each 10 μm in length and 4 μm in diameter), soma (single compartment, 50 μm in length and diameter), and a long "apical" dendrite (200 compartments, each 10 μm in length and 2 μm in diameter). Dendritic spines, each consisting of a cylindrical neck (0.4 μm in length, 0.25 μm in diameter) and a spherical head (0.5 μm in diameter), were attached to the first 1400 μm of the dendrite at a spacing of 50 μm. Each spine head contained a synapse with AMPA-Rs, NMDA-Rs, and VGCCs.

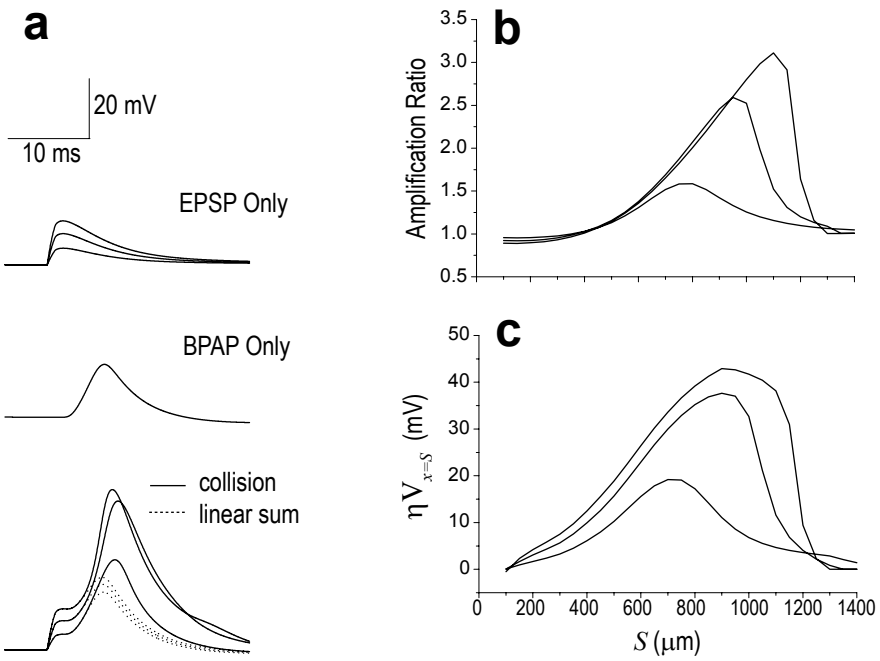

Figure 2.

(a) Voltage traces measured within a synaptic spine located 750 μm from the soma. Top traces show solitary EPSPs of 5 mV (AMPA=6 nS/μm^2; NMDA= 3.75 nS/μm^2), 10mV (AMPA=4 nS/μm^2; NMDA= 2.5 nS/μm^2), and 15 mV (AMPA=2 nS/μm^2; NMDA= 1.25 nS/μm^2). Middle trace shows BPAP alone. Bottom traces show collision of 5 mV, 10 mV, and 15 mV EPSPs with a BPAP (solid lines), compared to linear sum of EPSP and BPAP alone (dashed lines).

(b) Spatial distirbution of amplifcation ratio, measured at the site of the activated synapse (x-axis plots the distance, *S*, of the activated synapse from the soma).

(c) Spatial distribution of the voltage coincidence detection index, $\eta V_{x=S}$, measured (in mV) at the site of the activated synapse.

E_K=-90 mV, and E_{Ca}=120 mV. Rest potential was -72 mV, and the simulated temperature was 37ºC with kinetics scaled by Q10 of 4.0 as in Stuart and Häusser[2]. The integration time step was 25 μs.

Amplification of BPAPs by EPSPs

To begin each simulation, an EPSP of varying sizes (either 5, 10, or 15 mV) was initiated at a synapse in one of the spine heads. After a 1 ms delay, a BPAP was initiated by injecting a 2 nA current for 0.2 ms into the axon hillock of the postsynaptic cell, so that the BPAP and EPSP subsequently collided in the dendrite. A series of simulations was run, in which the EPSP was generated in spine heads that ranged between 100–1400 μm from the soma, in increments of 50 μm. In agreement with previous experiments and modeling results[1,2], collisions of the EPSP and BPAP often resulted in supralinear amplification of the BPAP at the activated synapse (see traces, Fig. 2a), due to activation of dendritic Na^+ channels. The degree of supralinear amplification can be quantified by the *voltage amplification ratio*, which is defined as the peak of the amplified BPAP divided by the peak of the linear sum of the EPSP and BPAP[2]. In our simulations, the amplification ratio increased as the activated synapse moved farther away from the soma, peaking at a distance of about 750 μm for a 5 mV EPSP, 1000 μm for a 10 mV EPSP, and 1100 μm for a 15 mV EPSP (Fig. 2b). Stuart and Häusser[2] have reported a similar spatial gradient of the amplification ratio in dendritic recordings from layer 5 pyramidal neurons, and they reproduced this phenomenon in a compartmental model. In our simulations, when the stimulated synapse was placed farther than ~1300 μm from the soma, the amplification ratio steeply decreased (Fig. 2b), because BPAPs decayed in amplitude as they traveled farther from the soma. Beyond ~1300 μm from the soma, the BPAP became so small that collision with a presynaptic EPSP no longer boosted it above threshold for activating dendritic Na^+ channels, hence no amplification occurred.

The Voltage Coincidence Detection Index

By definition, a coincidence detection signal should be switched on when the pre and postsynaptic cells are activated together, but not when either cell is activated alone. Therefore, the ability of amplified BPAPs to detect coincident spikes in the pre and postsynaptic cell depends on how large the peak voltage of the amplified BPAP is, compared to the peak voltage of an EPSP or BPAP occurring alone. This difference may be quantified by calculating a *voltage coincidence detection index*, which we define as

$$\eta V_x = V_x^{COLL} - \max(V_x^{EPSP}, V_x^{BPAP}), \qquad \text{[Eq. 1]}$$

where ηV_x is the voltage coincidence detection index measured at spatial position x within the cell, V_x^{COLL} is the peak value of V_m attained at position x during a collision-amplified BPAP, V_x^{EPSP} is the peak V_m attained at position

x during an EPSP alone, and V_x^{BPAP} is the peak V_m attained at position x during a BPAP alone. At a given location x within the cell, ηV_x measures the amount by which the peak V_m of an amplified BPAP exceeds the largest V_m that can be attained by an EPSP or BPAP occurring alone. Hence, ηV_x quantifies how well the peak V_m discriminates coincident pre and postsynaptic spikes from spikes that occur only in the pre or postsynaptic cell.

A coincidence detector that supports synaptic modification would be expected to reside at the location of the synapse to be modified. Therefore, we examined the value of ηV_x within the spine head containing the synapse that was activated during the simulation (we henceforth denote this synapse location as S, so that the coincidence detection index at this location may be denoted $\eta V_{x=S}$). We found that in our model, as S was moved farther from the soma, the value of $\eta V_{x=S}$ peaked at distance of S=675 μm for a 5 mV EPSP, S=900 μm for a 10 mV EPSP, and S=875 μm for a 15 mV EPSP (Fig. 2c). The largest values of $\eta V_{x=S}$ exceeded 40 mV, and $\eta V_{x=S}$ showed a spatial distribution similar (although not identical) to the amplification ratio.

Synapse Specificity of ηV_x

A coincidence detection signal should turn on when the pre and postsynaptic cells are activated together, and remain off when either cell is activated alone. But in addition, a Hebbian coincidence detection signal must also be synapse-specific, becoming activated only at those synapses in the postsynaptic cell where EPSPs occur concurrently with the postsynaptic spike. Stuart and Häusser[2] have presented a model of BPAP amplification in which the supralinear amplification of BPAPs was localized to a region of the dendrite surrounding the activated synapse. This suggests that if BPAP amplification supports a coincidence detection mechanism, then this mechanism may be reasonably well localized to active synapses. Here, we examined whether the voltage coincidence detection index, ηV_x, was well-localized to the stimulated synapse. To do this, we recorded the peak voltage of the amplified BPAP not only in the spine head of the activated synapse (as in Fig. 2), but in all other spine heads as well.

Fig. 3 shows a series of contour plots in which the somatic distance x of voltage measurements is plotted on the x-axis, the distance S of the stimulated synapse from the soma is plotted on the y-axis, and the shading of the contour (z-axis) indicates the voltage measurement within a spine (not necessarily the activated spine) at location x during the simulation. In these contour plots, synapse-specific signals lie on the $y=x$ diagonal, because this is where $x=S$ (the location x of the measurement equals the location S of the activated synapse). Thus, in these contour plots, signals that lie far from the diagonal are distant from the activated synapse, and therefore not synapse-specific.

Fig. 3a shows the spatial distribution of peak voltages generated by a single 5 mV EPSP occurring at varying distances from the soma, in the absence of any BPAP. Note that this voltage signal is "ideally" synapse-specific,

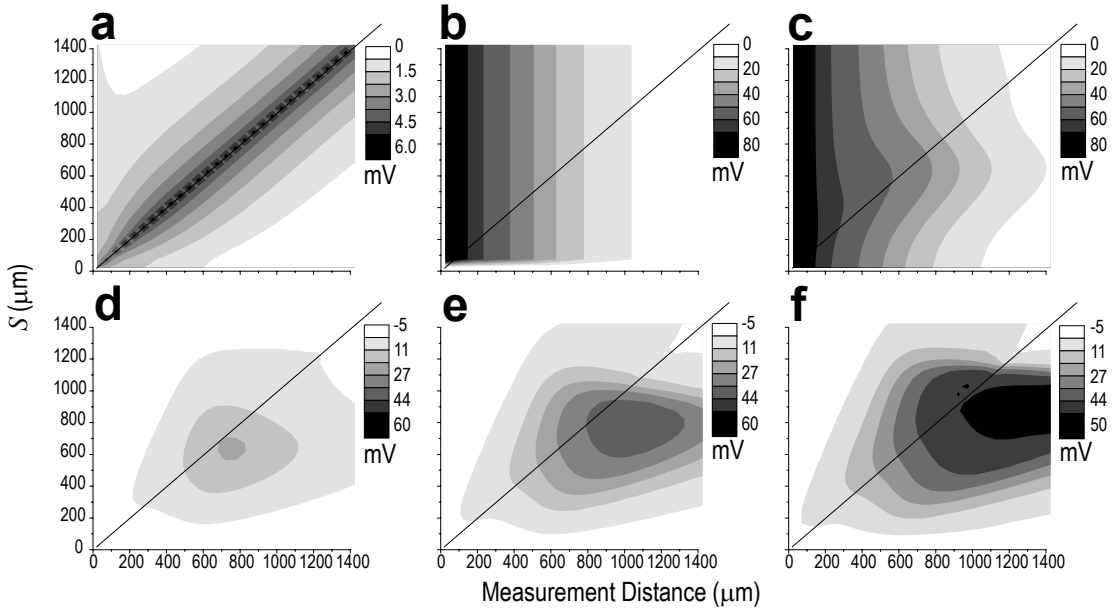

Figure 3. Synapse-specificity of V_m (a-c) and $\eta V_{x=S}$ (d-f). See text for explanation.

because the depolarization originates within the spine head of the activated synapse and dissipates into the surrounding dendrite. Thus, the contour plot exhibits a synapse-specific ridge along the diagonal. In contrast, Fig. 3b shows the spatial distribution of peak voltages generated when a BPAP occurs in the postsynaptic cell, and no EPSP occurs in any spine head. Unsurprisingly, this signal is not localized to any synapse, because no synapse is activated at all (and hence each horizontal cross-section of the contour plot is identical). Fig. 3c shows the spatial distribution of peak voltages generated when a BPAP collides with a 5 mV EPSP. The raw voltage signal plotted in Fig. 3c does not look synapse-specific, because the largest membrane depolarization occurs near the soma where the BPAP originates, rather than at the synapse where the BPAP and EPSP collide. However, it is not the raw membrane depolarization that quantifies the coincidence detection signal, but rather the difference between the voltage attained when the pre- and postsynaptic cells are activated together versus alone, which is measured by ηV_x.

Fig. 3d plots the spatial distribution of ηV_x for the collision between a BPAP and a 5 mV EPSP (following Eq. 1, this plot was generated by performing a pointwise subtraction of the contour plot in either Fig. 3a or 3b, whichever was larger, from the contour plot in Fig. 3c). It can be seen in Fig. 3d that ηV_x is largest for synaptic inputs between 650-800 μm from the soma. Over this narrow range of synaptic locations, the peak value of ηV_x lies near the diagonal, indicating that the coincidence detection signal is reasonably synapse-specific in these regions of the dendrite. However, the value of ηV_x spreads away from the diagonal at other values of *S*. This effect becomes even more pronounced as the EPSP increases to 10 mV (Fig. 3e) or 15 mV (Fig. 3f), because with larger EPSPs, the amplified BPAP propagates further into more distal regions of the dendrite, skewing ηV_x to the right of the diagonal. Therefore, ηV_x is only modestly synapse-specific for small EPSPs, and is even less synapse-specific for larger EPSPs. These results indicate that amplified BPAPs generally do not remain well localized to the region of the stimulated synapse. This finding seems to contradict the idea that a synapse-specific coincidence detection signal can be derived from supralinear amplification of the BPAP by EPSPs. However, before drawing this conclusion, it is necessary to examine how amplified BPAPs act to open VGCCs in different regions of the dendrite.

Ca^{2+} Entry Through VGCCs

It has been proposed that amplified BPAPs might support coincidence detection by opening VGCCs[1]. According to this theory, the amplified BPAP depolarizes the membrane sufficiently to open VGCCs, whereas the EPSP or BPAP alone do not cause sufficient depolarization to open VGCCs. Supporting this, BPAPs amplified by EPSPs have been shown to cause a greater influx of Ca^{2+} through VGCCs than do EPSPs or BPAPs by themselves[1]. Thus, VGCCs may act as coincidence detectors, since they are only opened when pre and postsynaptic spikes occur together, and not when either occurs alone.

VGCCs can be found in dendritic spines[12], so we inserted VGCCs into the spines of our model, to examine if they could function as coincidence detectors by opening selectively during the collision between a BPAP and an EPSP. To keep the membrane dynamics of the model as simple as possible, the peak conductance of the VGCCs was small (10 pS/cm^2), so that inward current through VGCCs did not have a large influence on V_m. In simulations, the membrane depolarization resulting from an EPSP alone did not approach near $V½_\alpha$, the half-maximal activation threshold for VGCCs, regardless of EPSP size (Fig. 4). Therefore, EPSPs alone did not trigger Ca^{2+} entry into synaptic spines. The membrane depolarization resulting from a BPAP alone exceeded $V½_\alpha$ in spines that were proximal to the soma (since the BPAP is very large in this region), but as the BPAP decayed in amplitude at increasingly distal spines, depolarization fell well below $V½_\alpha$, so that the BPAP alone caused very little calcium entry though VGCCs at non-proximal synapses (Fig. 4). However, in simulations where a BPAP collided with an EPSP, the peak of the amplified BPAP usually approached $V½_\alpha$ within the spine of the activated synapse, except when the activated synapse was very distal from the soma (circle symbols, Fig. 4b). Thus, unlike EPSPs or BPAPs alone, amplified BPAPs were able to open VGCCs sufficiently to allow Ca^{2+} entry into activated spines throughout much of the dendrite's spatial extent. The amount of Ca^{2+} entry was proportional to the size of the EPSP that collided with the BPAP, since larger EPSPs brought the peak of the amplified BPAP nearer to $V½_\alpha$, and thus caused more Ca^{2+} entry.

In summary, throughout most of the dendrite in our model, Ca^{2+} only enters the spine of an activated synapse through VGCCs when pre and postsynaptic cells are activated together, and not when either cell is activated alone. This is consistent with experimental evidence that VGCCs may function as Hebbian coincidence detectors[1,2].

The VGCC Coincidence Detection Index

The ability of VGCCs to detect coincident spikes in the pre and postsynaptic cell depends on the total amount of

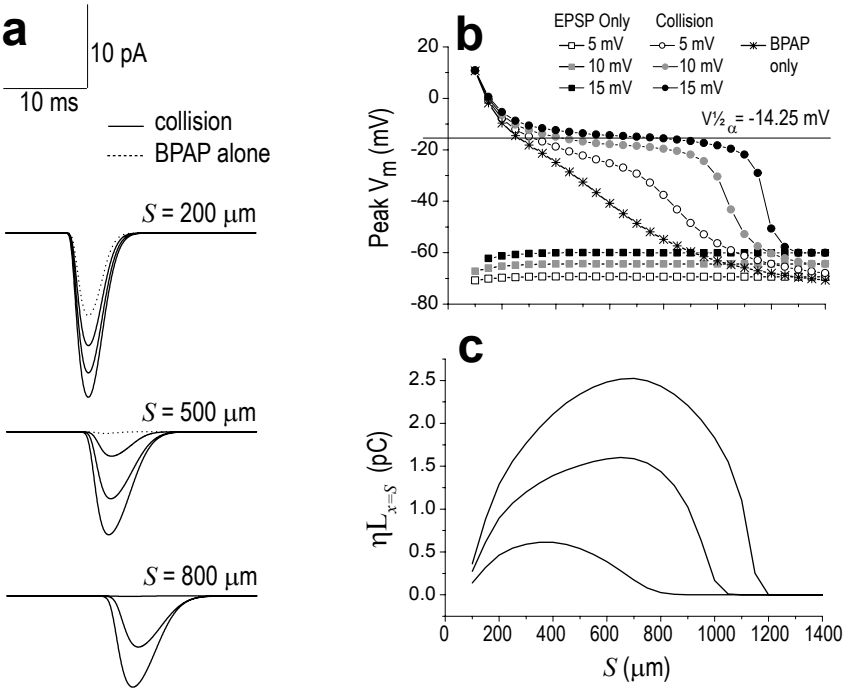

Figure 4.

(a) VGCC currents measured within a synaptic spine located 200 μm (top traces), 500 μm (middle traces), or 800 μm (bottom traces) from the soma. Notice that the BPAP alone (dashed traces) can only open VGCCs near the soma, but not at more distal locations.

(b) Spatial distirbution of peak V_m attained during the simulation, measured at the site of the activated synapse (x-axis plots the distance, *S*, of the activated synapse from the soma). Notice that beyond about 500 μm from the soma, a collision between a BPAP and EPSP is required to bring V_m near the activation threshold for VGCCs.

(c) Spatial distribution of the VGCC coincidence detection index, $\eta L_{x=S}$, measured (in pC) at the site of the activated synapse.

Ca^{2+} entry through VGCCs during the amplified BPAP, compared to the amount of Ca^{2+} entry during a solitary EPSP or BPAP. The amount of Ca^{2+} entry through VGCCs is proportional to the time integral of the VGCC Ca^{2+} current, which reflects the total Ca^{2+} charge transfer (measured in picocoulombs, abbreviated pC) into the cell through VGCCs during the simulation. Hence, the ability of VGCCs to function as coincidence detectors may be quantified by calculating a *VGCC coincidence detection index*, which we define (analogously to Eq. 1 above) as

$$\eta L_x = L_x^{COLL} - \max(L_x^{EPSP}, L_x^{BPAP}), \qquad \text{[Eq. 2]}$$

where ηL_x is the VGCC coincidence detection index measured at spatial position *x* within the cell, L_x^{COLL} is the VGCC charge transfer into the spine at position *x* during the collision-amplified BPAP, L_x^{EPSP} is the VGCC charge transfer into the spine at position *x* during the EPSP alone, and L_x^{BPAP} is the VGCC charge transfer into the spine at position *x* during the BPAP alone. At a given location *x* within the cell, ηL_x measures how much the VGCC charge transfer during an amplified BPAP exceeds the largest VGCC charge transfer that occurs during an EPSP or BPAP occurring alone. Hence, ηL_x quantifies how well the Ca^{2+} entry through VGCCs discriminates coincident pre and postsynaptic spikes from spikes that occur in either the pre or postsynaptic cell alone.

Synaptic plasticity is thought to be controlled by calcium entering the postsynaptic cell at the site of the activated synapse. Therefore, we examined the value of $\eta L_{x=S}$ in our model, which is the VGGC coincidence detection index at the site $x=S$ of the activated synapse. We found that in the model, the value of $\eta L_{x=S}$ peaked at distance of S=350 μm from the soma for a 5 mV EPSP, S=700 μm for a 10 mV EPSP, and S=700 μm for a 15 mV EPSP (Fig. 4c). Thus, the value of $\eta L_{x=S}$ has a spatial distribution rather similar to that of $\eta V_{x=S}$ (Fig. 2c), but shifted somewhat to the left. We will now show that ηL_x is considerably more synapse-specific than ηV_x.

Synapse Specificity of ηL_x

As explained above, a Hebbian coincidence detection signal must be synapse-specific. Thus, if VGCCs are to act as Hebbian coincidence detectors, it is not enough for $\eta L_{x=S}$ to be large. In addition, $\eta L_{x\neq S}$ must be small. That is, the coincidence detection signal should be present only at the activated synapse (position $x=S$), and absent at inactive synapses (positions $x\neq S$). Fig. 5 shows a series of contour plots (similar to Fig. 3) in which the shading of the contour (*z*-axis) denotes the local value of ηL_x within a spine at distance *x* from the soma. As explained above for Fig. 3, synapse-specific signals lie on the $y=x$ diagonal. Fig. 5a plots the spatial distribution of ηL_x for the collision between a BPAP and a 5 mV EPSP. The shaded region in Fig. 5a shows a moderate elevation of ηL_x near the diagonal at synaptic distances ranging from about 200-600 μm from the soma. This elevated region becomes broader and more pronounced as the size of the EPSP increases to 10 mV (Fig. 5b) or 15 mV (Fig. 5c), but remains

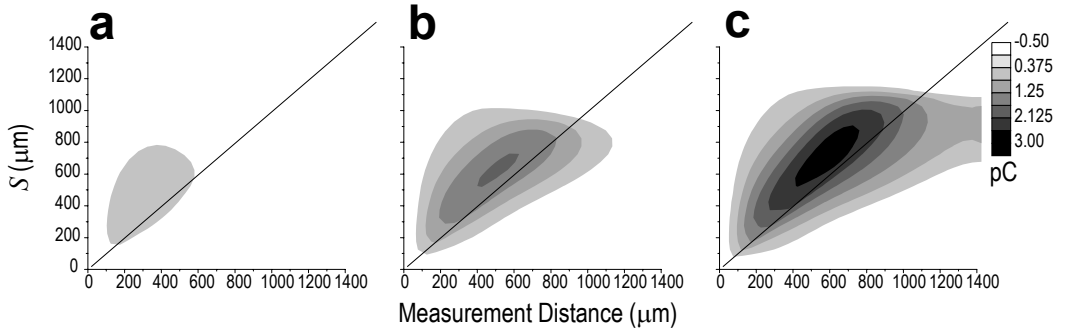

Figure 5. Synapse-specificity of $\eta L_{x=S}$ for collision of a BPAP with a 5 mV (a), 10 mV (b), or 15 mV (c) EPSP. See text for explanation.

near (albeit slightly to the left of) the diagonal. Indeed, for the 15 mV EPSP (Fig. 5c), robust coincidence-triggered Ca^{2+} elevation occurs over ~1000 μm of the dendrite's spatial extent, and is reasonably well restricted to the region of the activated synapse (since it lies near the diagonal). These results lend support to the idea that VGCCs may be able to function as synapse-specific coincidence detectors.

Conclusions

We have shown that the amplified dendritic voltage signal which occurs when a BPAP collides with an EPSP is poorly localized to the synapse where the EPSP is generated (Fig. 3). Nonetheless, the activation of VGCCs by this voltage signal is better localized to the region of the input synapse than the amplified BPAP itself (Fig. 5), due to spatial filtering of the voltage signal by the VGCC activation threshold (Fig. 4). It is important to recognize that the synapse specificity of VGCC activation (which spans a region ~200 μm on either side of the active synapse) cannot approach the specificity of NMDA receptor activation (which is confined to the spine of the activated synapse). However, it is possible that the synapse specificity of the VGCC Ca^{+} signal could continue to improve at later stages of molecular signaling. Thus, just as VGCCs can spatially filter V_m to improve synaptic localization of coincidence detection by amplified BPAPs (as we have shown), the activation of second messengers by VGCC Ca^{+} entry might spatially filter the signal again, further improving synaptic specificity of the coincidence detection signal. After several stages of a molecular cascade, such signals might approach the synapse-specificity of NMDA currents.

Our present findings imply a "center-surround" pattern of Ca^{+} entry when pre- and postsynaptic spikes occur together, since activation of NMDA receptors is centered on the active synapse, and activation of VGCCs surrounds the active synapse. A possible functional consequence of this could be spatial competition for potentiation among neighboring synapses, especially if NMDA receptors are needed for synaptic potentiation, whereas activation of VGCCs alone causes synaptic depression[13]. Alternatively, activation of VGCCs surrounding the active synapse might trigger spine outgrowth[14], to reach additional sources of axonal input located near the active synapse. Further study is needed to explore the functional implications of regionally localized coincidence detection byVGCCs.

References

[1] Magee JC & Johnston D, *Science* 275:209-213, 1997.
[2] Stuart GJ & Häusser M, *Nature Neuroscience* 4:63-71, 2001.
[3] Hebb D, *The Organization of Behavior*. New York: John WIley and Sons, 1949.
[4] Bliss TVP & Collingridge GL, *Nature* 361:31-39, 1993.
[5] Aniksztejn L & Ben-Ari Y, *Nature* 349:67-69, 1991.
[6] Grover LM & Tyler TJ, *Nature* 347:477-479, 1990.
[7] Weisskopf MG, Bauer EP, LeDoux JE, *Journal of Neuroscience* 19:10512-10519, 1999.
[8] Mainen ZF, Joerges J, Huguenard JR, Sejnowski TJ, *Neuron* 15:1427-1439, 1995.
[9] Destexhe A, Mainen ZF, Sejnowski TJ, Neural Computation 6: 10-14, 1994.
[10] Destexhe A, Mainen ZF, Sejnowski TJ, In: Methods in Neuronal Modeling (2nd edition; edited by Koch, C. and Segev, I.), MIT press, Cambridge, 1996.
[11] Mermelstein PG, Bito H, Deisseroth K, Tsien RW, *Journal of Neuroscience* 20:266-73, 2000.
[12] Sabatini BL & Svoboda K, *Nature* 408:589-93, 2000.
[13] Christie BR, Schexnayder LK, Johnston D, *Journal of Neurophysiology* 77:1651-1655.
[14] Bonhoeffer T & Yuste R, *Neuron* 35:1019-1027, 2002.